Computers and Geotechnics 84 (2017) 117–128

Contents lists available at ScienceDirect

Computers and Geotechnics

journal homepage: www.elsevier.com/locate/compgeo

Research Paper

A network model to assess base-filter combinations

T. Shire *, C. O'Sullivan

Department of Civil and Environmental Engineering, Imperial College London, South Kensington, London, UK

ARTICLE INFO

Article history:
Received 30 January 2016
Received in revised form 16 November 2016
Accepted 21 November 2016
Available online 7 December 2016

Keywords:
Network model
Granular filter
Internal erosion
Voids
Constrictions

ABSTRACT

Granular filters retain base material within the narrowest constrictions of their void network. A direct comparison of the base material particle size distribution (PSD) and the filter constriction size distribution (CSD) cannot easily be used to assess filter-base compatibility. Here a conceptually simple random-walk network model using a filter CSD derived from discrete element modelling and base PSD is used to assess filter-base compatibility. Following verification using experimental data the model is applied to assess empirical ratios between filter and base characteristic diameters. The effects of filter density, void connectivity and blocking in the first few filter layers are highlighted.

1. Introduction

Granular filters play an important role in many geotechnical structures, most notably embankment dams and flood embankments. As outlined in [1] filters downstream of the core can interrupt or halt internal erosion by trapping mobile particles that are entrained in seeping water. The function of a filter (usually comprising a sand or gravel) is to retain a finer base material. Hitherto, filter design has been largely empirical, with consideration of the particle-scale mechanisms based on intuition and highly idealized models. It is generally accepted that both the filter constriction sizes (i.e. the sizes of the pore throats or narrowest points in the void space) and the particle size distribution (PSD) of the finer base material determine whether a base material will be retained in a given filter i.e. the filter and base will be compatible. A representative filter particle size is generally taken to indicate the filter constriction sizes [2]. The development of micro-computed tomography (μCT) and the discrete element method (DEM) mean that the constrictions within a granular material can now be quantified. If both the base PSD and the filter CSD are known and if there is an overlap in the range of sizes covered by each, a simple visual comparison of the distributions will not always indicate whether a filter will prevent unacceptable erosion of base material.

This contribution aims to advance understanding of filter behaviour by using a network-based analysis approach to assess base-filter combinations where the filter CSD is known. The conceptually simple network model uses an area-biased random walk algorithm. CSD data are generated by applying the weighted Delaunay triangulation approach proposed by Reboul et al. [3] to virtual samples created using the discrete element method (DEM). The network model's performance is verified using simple base-filter combinations and experimental data [4]. The "no", "some" and "continuing" base soil erosion categories proposed by Foster and Fell [5] are revisited and the network model is used to explore the filter mechanics in some detail.

2. Background

The classic filter rule proposed by Terzaghi defines an effective filter, i.e. a filter that can retain a given base material, as one with $D_{15F}/D_{85B} \leqslant 4$, where D_{15F} is the filter particle diameter for which 15% of the material by mass is finer and D_{85B} is the base particle diameter for which 85% of the material by mass is finer [6]. In developing this rule, Terzaghi proposed that the characteristic filter particle diameter D_{15F} be considered as a proxy for a characteristic diameter of the constrictions within the filter void network [2] and this concept has been adopted in subsequent studies. In their experimental work, Kenney et al. [4] found that $D_c^* \leqslant D_{15F}/5$ (where D_c^* is the controlling constriction size, taken to be equal to the largest eroded particle) and they advocated the continued use of the Terzaghi relationship. Sherard and Dunnigan [7] also recommend D_{15F} as a characteristic filter diameter for design, but to vary the D_{15F}/D_{85B} ratio depending on the base material being assessed.

For ageing dams with filters which were not designed to meet modern filter requirements, rather than drawing a distinct line

* Corresponding author.
E-mail address: thomas.shire09@imperial.ac.uk (T. Shire).

http://dx.doi.org/10.1016/j.compgeo.2016.11.014
0266-352X/

between "effective" and "ineffective" filters, Foster and Fell [5] proposed categorizing filters as follows: (i) "seal with no erosion" where very little material is passed through the filter or is eroded (ii) "seal with some erosion" (iii) "partial or no seal with large erosion" or "continuing erosion" where the filter is too coarse for the base material to seal the filter. As with the Sherard and Dunnigan [7] criteria, the boundary between no erosion and some erosion depends on the base soil under consideration. For base soils with less than 15% cohesive fines, this boundary is drawn at $D_{15F}/D_{85B} \leqslant 7$. For the some/continuing erosion boundary, D_{95B} was found to be a more effective base soil parameter than D_{85B}, and the boundary was drawn at $D_{15F}/D_{95B} \leqslant 9$. The use of relatively large base particles for the characteristic base diameter (i.e. D_{85B} or D_{95B}) shows that the rules implicitly take into account the process of self-filtering, where coarser transported base particles first block the constrictions of the filter and therefore prevent the loss of the finer base particles [8]. This is distinct from clogging of the filter, which Vaughan and Soares [8] defined as "a slow blocking of the filter... generally indicates eventual stability".

DEM enables creation of virtual samples and the particle scale data generated can be analysed to generate a CSD [3,9,10]. It is also now possible to use μCT to directly image filters and algorithms to generate a CSD have been proposed [11–13]. While the availability of filter CSD data enables a more detailed scientific assessment of filter-base interactions, direct comparison with the base PSD reveals little about the filter performance. Analyses that consider the dynamic nature of the filter-base interaction are needed and here a network-based approach is adopted.

3. Network-based model

Network models to consider pore-scale flow in porous media comprise nodes representing void bodies connected by tubes or bonds that represent the narrowest connecting constrictions or pore throats. This simplified network structure considers only which voids are connected, and the diameter of the narrowest connecting constriction, as shown schematically in Fig. 1. Jang et al. [14] give a general overview of the use of network models in fundamental studies of permeability, multiphase flow and resource recovery. Prior studies that have applied network modelling to study filtration include [15–17]. Many of the network models used to date consider the networks to be arranged as a regular lattice of bonds and nodes, e.g. [14,16]. Following Schuler [18] recent research on granular filters has concentrated on the use of regular cubic networks, i.e. each void has six connections with other voids, one downstream, one upstream and four sideways, e.g. [16,19]. The regular cubic network is justified based on an experimental study reported by Witt [20], who measured pore and constriction distributions in resin-impregnated gravel samples and found an average of 5.7 constrictions per pore body. In Schuler's model the network constrictions are assumed to have randomly assigned diameters to match the CSD. Assuming that each base particle which infiltrates the network is able to infiltrate in either the sideways or downstream directions (i.e. each void has 5 exits, one downstream and 4 sideways). The number of downstream layers through which a base particle of a given diameter can infiltrate can be probabilistically calculated using:

$$n = \frac{\ln(1-\bar{P})}{\ln(P(F))} \tag{1}$$

where $P(F)$ is the probability of a particle moving one layer downstream and $\bar{P}$ is a confidence interval, typically set between 95% and 99%. $P(F)$ is the probability of a particle making a downstream step through the network, which is a function of the probability of a base particle passing through a single constriction. More details on the calculations can be found in [19]. Sjah and Vincens [16] also used this model to back-calculate a CSD curve from experimentally derived number of filter layers through which base particles may infiltrate. A drawback of the probabilistic network model is that it considers the infiltration depth of single particles only. Blocking of constrictions within the filter network and the effect of these blockages on the retention of finer base is not explicitly considered. Semar [21] presented a network model for granular filters to explicitly consider the full CSD. Constrictions were randomly assigned to an initially cubic network to match the CSD. All constrictions smaller than a specified base particle diameter were deleted. If the resulting network percolated (i.e. if there was a continuous path from one side of the filter to the other [22]), the base particle was taken to be susceptible to erosion. As with the probabilistic model, only a single base diameter is considered by a single network simulation. Locke et al. [19] presented a time-dependent model based on a cubic network. Moraci et al. [23] presented a method to predict suffusion using a layer-based model that considers alternate layers of particles and constrictions [23] where the CSD is obtained using the Silveira method [24].

Here a new network model is proposed which is able to account for a polydisperse base PSD and can therefore model the processes of clogging and self-filtering. The model simulates the inter-void movement of particles matching the base PSD using a timestepping, area-biased random walk algorithm. The regular cubic network topology adopted by previous researchers in the field of granular filters is adopted here, as shown schematically in Fig. 2.

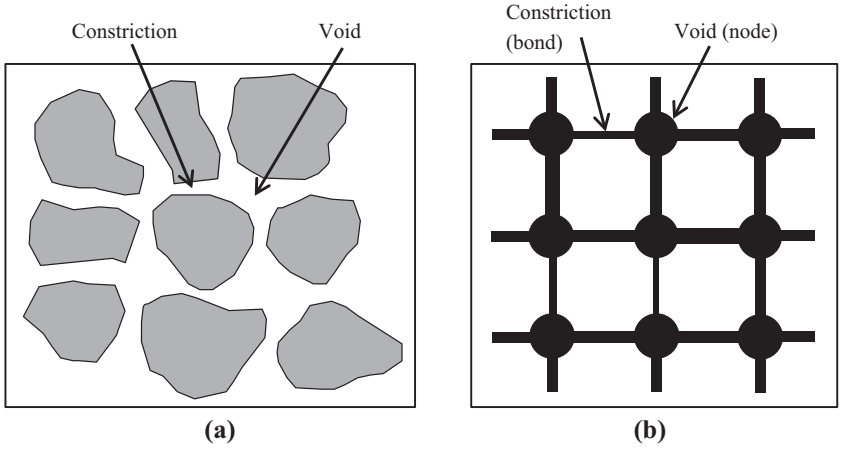

Fig. 1. (a) Schematic diagram of void fabric; (b) representation of void fabric in a network model.

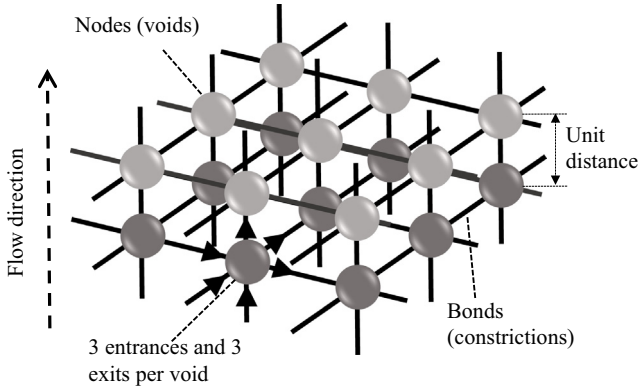

Fig. 2. Network structure.

At the boundaries, the network has start and end nodes in the direction of flow, and is periodic in the directions perpendicular to flow. The sizes of the cylindrical bonds in the network are specified to match a particular CSD. The network is "directed" and the particles can move only in the positive Cartesian directions, i.e. each internal void has three entrances (one upstream and two sideways) and three exits (one downstream and two sideways), as shown schematically in Fig. 2. This is in contrast to the cubic network used in Eq. (1), in which it is assumed that particles may both enter and exit voids through each of the sideways constrictions, or the Moraci et al. method [23] where the particles move in only one direction. A unit spacing is adopted between nodes, representing the distance between neighbouring voids. Sjah and Vincens [16] considered this spacing and concluded that D_{50} of the filter PSD by number gave the best estimate.

An area-biased random walk algorithm, developed with reference to [17], was used to simulate the passage of a finer, base material through the network. The main steps of the algorithm are set out in Fig. 3. Spherical base particles selected to match the base PSD are introduced to the start nodes along one external face of the filter (as illustrated schematically in Fig. 2). For each simulation the number of base particles which are inserted into the filter, N_{base}, is calculated by specifying the mass ratio of base material to filter material, F_{base}. N_{base} is then given by:

$$N_{base} = F_{base}\frac{N^{p}_{DEM}N_{nodes}}{N^{voids}_{DEM}}\frac{N_{base,unit}}{N_{filter,unit}} \quad (2)$$

where N_{voids} is the number of nodes (voids) in the network model, N^{p}_{DEM} and N^{voids}_{DEM} are the number of particles and voids in the DEM model used to determine the CSD and $\frac{N_{base,unit}}{N_{filter,unit}}$ is the ratio of the number of base particles per unit mass to the number of filter particles per unit mass, determined from the PSDs.

In the simulations presented here the total volume of base particles generated was 5% of the filter particle mass. However for the largest D_{15F}/D_{85B} ratio and the most widely graded base material values 10^9 finer base particles would be needed to match 5% of the filter particle mass. In these cases memory constraints restricted the total number of finer particles to be $\leqslant 2 \times 10^8$ particles per simulation.

The base particles move through the filter until they are retained or eroded (reach the end nodes), i.e. base particles can exist in one of three states: (i) still in motion; (ii) retained within the filter; (iii) eroded through the filter. During each increment each particle which is free to move attempts to move to a neighbouring void. The probability of one of the exit constrictions being selected to convey the particle to the next neighbouring void is proportional to the cross-sectional area of the exit constriction (Fig. 4), where only unblocked constrictions are considered. The cross-sectional area was selected on the basis of Poiseuille's law for flow through circular tubes, in which the maximum flow velocity is proportional to the tube radius squared.

As illustrated in Fig. 5, there are three possibilities for a given particle:

(a) If the particle diameter is smaller than the constriction diameter it is moved to the neighbouring void.
(b) If the particle diameter exceeds the constriction diameter, the particle is "retained" and the constriction is "blocked". The blocked constriction cannot be used to facilitate inter-void particle movement in subsequent increments.
(c) If all exits to a void are blocked, the particle is "retained". Note that there is no limit on the number of base particles which can enter a given void.

As illustrated in Fig. 3, the simulation progresses until all fines in the system can be classified as being either retained or eroded. The algorithm progresses incrementally. The base particles were added incrementally as in the real scenario base materials progressively erode and thereby gradually migrate into the filter. In each increment 1% of the total number of base particles to be considered are introduced to the network, until all of the base particles have been introduced.

Determining the minimum size of the network required to get results that were independent of the network size was an important step in the network model development. This was done through consideration of the percolation threshold [22]. A directed network can be considered to be percolating if there is a continuous path from the start to end nodes (i.e. sufficient constrictions/bonds are unblocked/open to allow a continuous path of open constrictions to exist between the start and end of the filter). In an infinitely large network, the point of percolation is well defined and it will always occur at the same fraction of open bonds [22]. The percolation threshold is the proportion of bonds that must be open in the network so that percolation is achieved. Networks of different sizes with all bonds initially closed were simulated and bonds randomly opened until the minimum percentage of bonds which needed to be open (i.e. unblocked) to allow percolation was determined. This was repeated 100 times for each network considered (networks of up to $80 \times 80 \times 80$ nodes were considered). Fig. 6 illustrates the standard deviation of the percolation thresholds for the networks considered; there is a clear decrease in the rate of reduction of the standard deviation when networks larger than $40 \times 40 \times 40$ nodes are considered. Based on these data a network with $40 \times 40 \times 60$ nodes (total 96,000 nodes), with 60 nodes in the direction of flow was used in the remainder of the simulations discussed here. Each network simulation took between two hours and four days using a HP Z600 workstation with 8 GB RAM, depending on the number of base particles used in the simulation.

The key advantages and limitations of the model are summarised in Table 1. A key advantage of the current model over previously proposed models [15,16] is that it can consider base materials with a range of PSDs and filter materials with a range of CSDs. Direct input of the filter CSD enables variations in the CSD with filter PSD and density to be considered. The blocking mechanism captured in this model is not included in prior models (e.g. it is absent from the Moraci et al. layer-based model) [23]. Up to 200 million base particles can be accommodated. Network statistics such as the PSDs of retained and eroded material and proportion of bonds blocked can easily be extracted at each time. It should be noted that in the current model formulation each model increment does not correspond to a specific time interval, but rather the increments allow filtration to progress until all the base material is accounted for. Nevertheless, the model will give

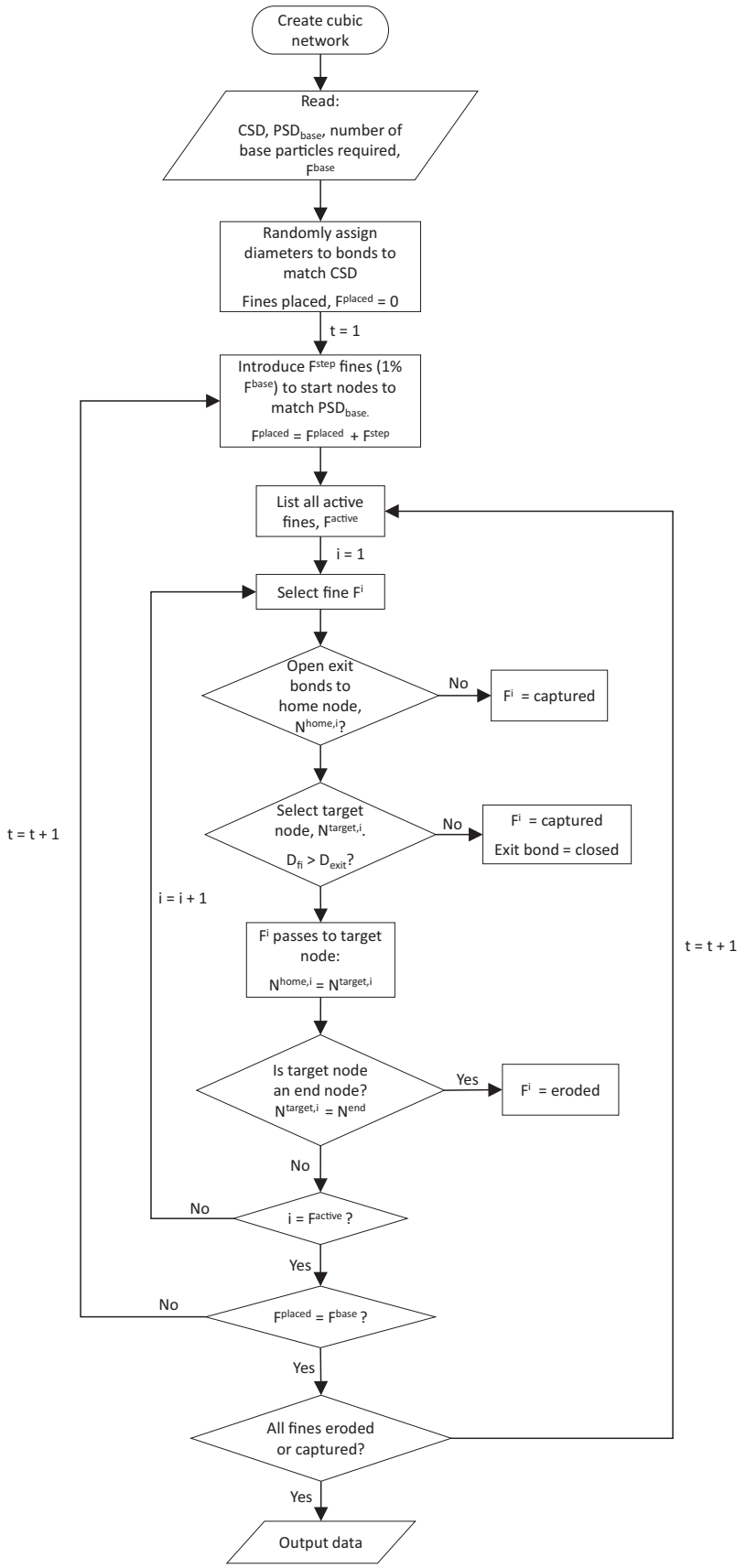

Fig. 3. Process involved in biased random walk model.

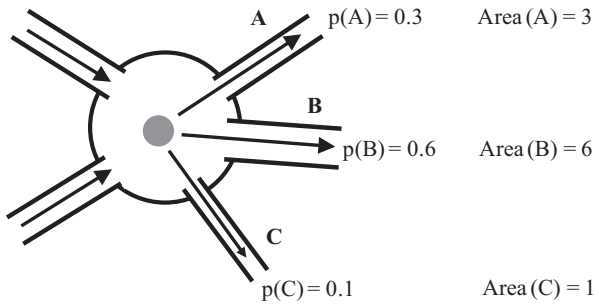

Fig. 4. Area-biased random walk simulation. The probability of a particle choosing a constriction is proportional to the constriction's area.

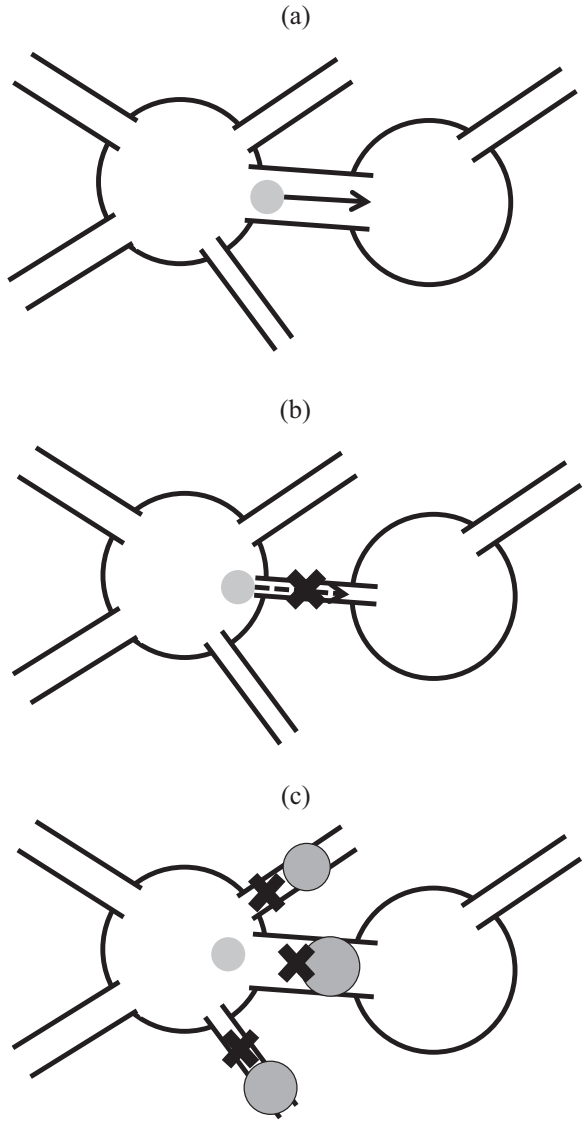

Fig. 5. Options for base particle movement or retention. (a) Base passes through constriction; (b) base is retained in constriction, constriction becomes blocked; (c) all exits are blocked and the particle is retained in the void.

information about how filtration will progress to a steady state (e.g. will self-filtration occur without significant erosion?). The model is highly ideal, for example the hydraulic conditions in the filter are not considered although these will influence the transport of particles and therefore the results should be treated

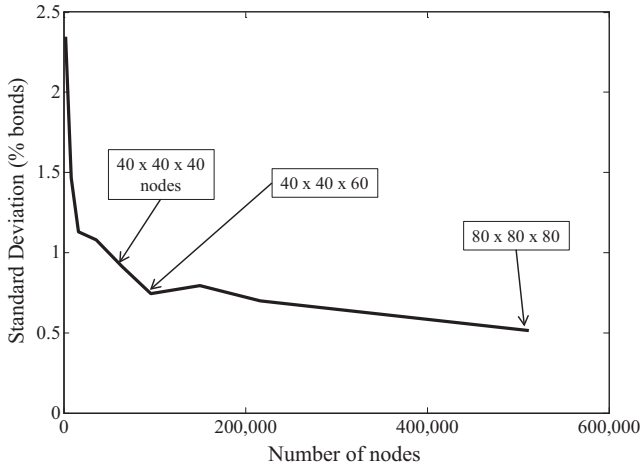

Fig. 6. Standard deviation of percolation threshold over 100 simulations for directed cubic networks of increasing size.

Table 1
Advantages and limitations of network model.

Advantages	Limitations/simplifications
• Can accommodate base and filter materials of varying PSD, so can simulate self-filtering • Uses a large number of particles (up to 200 million) • Uses calculated filter CSD, so automatically takes into account filter properties such as relative density • Network statistic such as backbone fraction can be collected • Can accommodate filter networks of varying structure (i.e. inter-void connectivity)	• Requires CSD calculation to be carried out • Hydraulic conditions are accounted for using a very ideal area bias assumption • Simplified void clogging process: no reduction in size due to clogging (constrictions either open with full diameter, or clogged) • Only single-particle retention considered. Other mechanisms e.g. particle bridging are not considered • Assumption that all base particles will enter the filter may not be valid for all base materials • Current cubic network assumption may not be realistic

as conservative. The complexity of flow through real filters was shown by computational fluid dynamic (CFD) simulations on microcomputed tomographic images of real filter sands by [25]. Flow through an individual constriction depends on its diameter, the local (micro-scale) hydraulic gradients and on its orientation with respect to the overall (macro-scale) hydraulic gradient direction, where constrictions within ±90° of the overall hydraulic gradient have the potential to allow particles to pass, but the fluid velocity reduces as the difference between the constriction orientation and the overall flow direction increases. Rege and Fogler [17] idealized the network as a 2D pipe network to calculate the flow between voids; for a 3D network representing a granular filter this would significantly increase the computational cost of the model and would still be a gross idealization of a system that has highly complex flow geometries.

4. DEM simulations to determine CSD for model application

To apply the model in the current study, DEM simulations were used to generate virtual filter samples with specific PSDs from which CSDs could be measured. The DEM simulations used to create the virtual granular filters used a modified version of the molecular dynamics code LAMMPS [26]. The specific simulation approach used here is discussed in [27]. To achieve homogeneity

a periodic cell was used in the simulations and the particles were initially randomly placed in the periodic cell. This initially loose, non-contacting assembly was isotropically compressed to a mean effective stress of p′ = 50 kPa, where p′ is the mean normal stress. Referring to Fig. 7(a) and Table 2, for all of the cases discussed here linear filter PSDs were considered, with coefficients of uniformity of the filter, $Cu_{filter} = D_{60F}/D_{10F}$ = 1.2, 1.5 and 3. The sample density was controlled by varying the inter-particle coefficient of friction (μ) applied during compression and the resultant void ratios for "loose" (μ = 0.3) and "dense" (μ = 0.0) samples are given in Table 2. Once the samples have reached p′ = 50 kPa the friction is changed to μ = 0.3, causing a very small amount of rearrangement, so that all samples have comparable characteristics. Note that the terms "loose" and "dense" do not correspond to the relative density calculated from laboratory tests using e_{max} and e_{min}. However, a DEM sample created with μ = 0.0 can be considered the densest possible and μ = 0.3 was selected to approximately match experimentally derived value of interparticle friction for glass beads [28], meaning that the sample compressed with μ = 0.3 can be considered loose. For all samples with $Cu_{filter} \leqslant 3.0$ it was possible to match the experimental void ratios of Kenney et al. [4] with $\mu \leqslant 0.3$. However, for the sample with Cu_{filter} = 6.0 the highest reasonable coefficient of friction of μ = 0.7 was used in order to create the loosest possible sample. This still resulted in a void ratio slightly higher than the experimental values (e_{LAB} = 0.39 – 0.43 and e_{DEM} = 0.34), however this was still considered reasonable for comparison purposes.

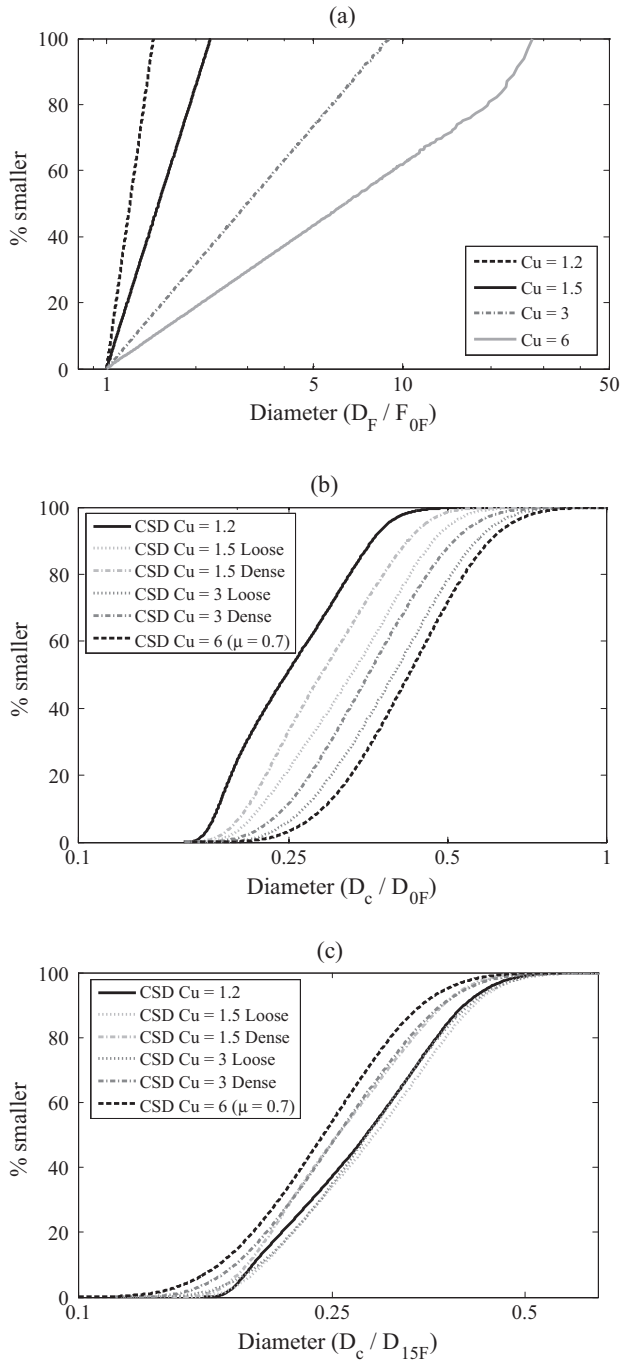

Fig. 7. Filter PSDs and corresponding CSDs used in network model. D_F is a filter particle diameter and Dc is a constriction diameter. Samples Cu = 1.2, Cu = 3.0 Dense, and Cu = 6 are equivalent to those considered in experiments by Kenney et al. [4].

The number of particles in the simulations increased with Cu_{filter} from 8262 (Cu_{filter} = 1.2) to 59,183 (Cu_{filter} = 6.0). As discussed in [29], once a stable system configuration was attained at p′ = 50 kPa, the constriction sizes were determined using the weighted Delaunay algorithm that was proposed by Reboul et al. [3]. This algorithm uses a weighted Delaunay triangulation of the particle centroids and the constriction sizes are determined by considering the maximum sized particles that can pass between the three particles that define each face in the tetrahedral system. Larger constrictions are considered to represent an over segmentation of the void space, and as discussed by [30], a user-controlled merging step is applied that effectively considers the overlap of the inspheres in adjacent tetrahedra; here a 50% overlap was used as the merging criterion. The resultant constriction size distributions (CSDs) are illustrated in Fig. 7(b) and (c) as cumulative distributions by number, while Table 2 indicates the coefficient of uniformity of the CSDs. Referring to Fig. 7, the effectiveness of any of these filters to retain a finer material cannot simply be determined by visual comparison of the finer PSD with the filter CSD. The CSD calculation (DEM simulations and CSD calculations) took between two days and three weeks, depending on the number and coefficient of uniformity of the DEM particles.

5. Validation of network model

The model was firstly validated by checking that monosized base particles equal to D_{c1} or $D_{c1.5}$, where *x*% of the total number of constrictions are smaller than D_{cx} caused blocking of 1 or 1.5% of the bonds.

Reference was then made to Kenney et al. [4] which includes data for hydraulic filter experiments that are well suited to verify the proposed model as a cohesionless base material was tested and the filter PSDs and void ratios and the largest eroded base particle diameter were given. Other experimental data [8,31–36] either used cohesive base materials or did not provide all the necessary data.

The materials considered by Kenney et al. [4] included both spherical glass beads and natural sands and gravels. Kenney et al. [4] found that when a finer base material with $Cu_{base} = D_{60B}/D_{10B}$ = 1.2 was considered, the largest base particles that could erode through filters with Cu_{filter} = 1.2, Cu_{filter} = 3.0 and Cu_{filter} = 6.0 had diameters approximately equal to $0.18D_{0F}$, $0.25D_{0F}$ and $0.26D_{0F}$ respectively.

DEM filter samples were created with similar PSDs (Cu_{filter} = 1.2, 3.0, and 6.0) to the filters tested by Kenney et al. [4]. For the cases with Cu_{filter} = 1.2 and Cu_{filter} = 3.0 the DEM samples had void ratios of e_{DEM} = 0.558 and e_{DEM} = 0.455 respectively; in both cases these values were within the range of the experimental void ratios, e_{LAB} (where Cu_{filter} = 1.2, $0.52 < e_{LAB} < 0.56$, and where Cu_{filter} = 3.0, $0.43 < e_{LAB} < 0.47$). For Cu_{filter} = 6.0 the DEM sample had e_{DEM} = 0.34

Table 2
Filter simulations for constriction size distributions.

Coefficient of uniformity, Cu_{filter}	Number of particles	Interparticle friction coefficient, μ	Void ratio at p′ = 50 kPa, e	Coefficient of uniformity of the CSD, Cu_{CSD}
1.2	8262	0.0	0.558	1.48
1.5	9313	0.0	0.531	1.52
		0.3	0.658	1.63
3	22,600	0.0	0.382	1.57
		0.3	0.455	1.60
6	59,183	0.7	0.340	1.57

and it was slightly denser than the experimental samples which had $0.39 < e_{LAB} < 0.43$. The DEM PSDs and resultant CSDs are included in the data presented in Fig. 7(a) and (b). The CSDs derived from the three DEM samples were used to create network models. For each network model a parametric study was then carried out using base materials with $Cu_{base} = 1.2$ where the ratio D_{50B}/D_{0F} was systematically incremented. The values of D_{50B}/D_{0F} considered were within a range of $0.1 < D_{50B}/D_{0F} < 0.4$ to enable consideration of progression from complete erosion to perfect filtration as indicated in Figs. 8–10. For each value of D_{50B}/D_{0F} the random walk algorithm was applied to the network model and the largest particle eroded and proportion of base material eroded were recorded and these values are compared with the experimental data in Figs. 8–10. The data presented in Fig. 8 indicate a very good agreement between the filter simulation results and the experimental data for $Cu_{filter} = 1.2$; the largest particle that passes through the filter is approximately $0.18D_0$ for all D_{50B}/D_{0F} ratios $\leqslant 2$, and the amount of material that passes through the network model drops significantly between $D_{50B}/D_{0F} = 0.15$ and $D_{50B}/D_{0F} = 0.18$. Referring to Figs. 9 and 10 for $Cu_{filter} = 3.0$ and 6.0 the agreement is reasonable. In both cases in the experiments the largest particle that passed through the filter was about $0.25D_0$; the network model predicted the largest particle passing through the filter to be $0.3D_0$ for $Cu_{filter} = 3.0$ and $0.34D_0$ for $Cu_{filter} = 6.0$. For these two filter models there is a significant decrease in the volume of base material that can pass through the filter between $D_{50B}/D_0 = 0.2$ and $D_{50B}/D_0 = 0.3$, with almost all the base material being retained by the filters at $D_{50B}/D_{0F} = 0.3$. The overall good agreement between the model results and the experimental data enables application of the model with confidence to analyse various base-filter combinations.

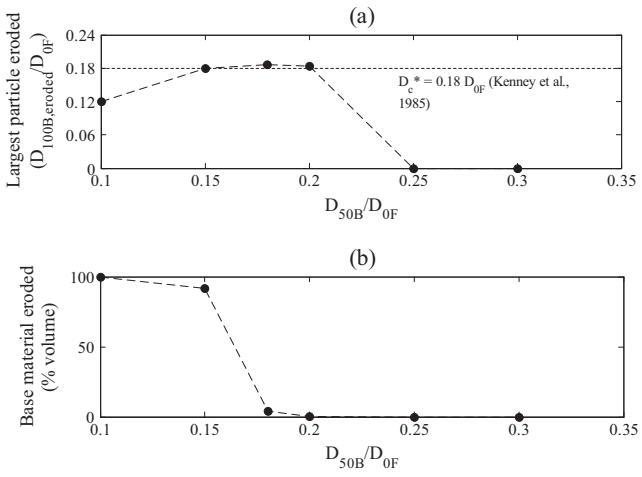

Fig. 8. Validation of random walk algorithms against experimental data of Kenney et al. (1985): filter Cu = 1.2. (a) Largest base particle eroded; (b) proportion of base material eroded.

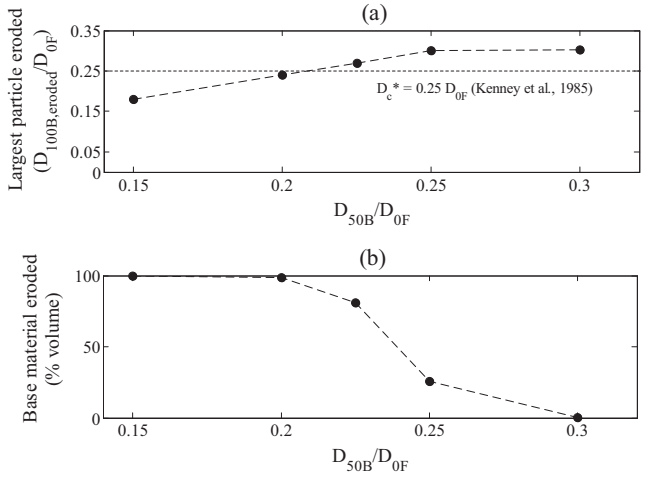

Fig. 9. Validation of random walk algorithms against experimental data of Kenney et al. (1985): filter Cu = 3.0. (a) Largest base particle eroded; (b) proportion of base material eroded.

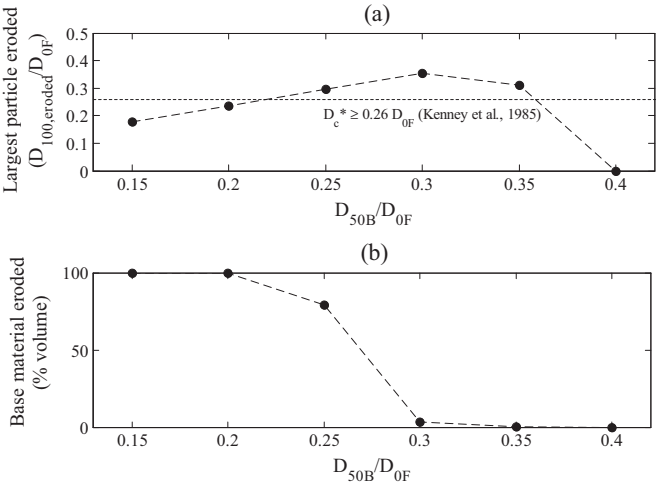

Fig. 10. Validation of random walk algorithms against experimental data of Kenney et al. [4]: filter Cu = 6.0. (a) Largest base particle eroded; (b) proportion of base material eroded.

6. Application of model to assess base/filter combinations

Having established the ability of the model to generate reasonable results, the model was applied to revisit the Foster and Fell [5] categorization of erosion. In this study 66 combinations of filters with finer base materials were considered. Referring to Fig. 7 and 4 filter scenarios were selected, with $Cu_{filter} = 1.5$ and $Cu_{filter} = 3.0$, each in a dense and loose state, with the resultant CSDs given in Fig. 7(b). For the finer base materials, three linear PSDs with

Cu_{base} = 1.5, 3 and 4.5 were considered as illustrated in Fig. 11. The size of the finer base particles was selected by setting D_{85B} equal to D_{c5}, D_{c10}, D_{c15}, D_{c25}, D_{c50} and D_{c75} of the CSD from the loose DEM sample for a given Cu_{filter} value. These sizes were used with both loose and dense filters so that the ratios D_{15F}/D_{85B} were the same. For the case of Cu_{filter} = 1.5, base materials with $D_{85B} = D_{c0}$ were also considered.

As described in Fig. 12, the simulations were carried out in two stages. In each stage the number of base particles was calculated using Eq. (2) or the limit of 200 million (i.e. a total of 400 million base particles was analysed for a single base-filter combination). The majority of constriction blockage occurred during the first stage. During the second stage (which uses the partially blocked network from the first simulation) the number of new constrictions which become blocked is significantly lower (typically around 10% of the first simulation). The second simulations was therefore used to assess the effect of constriction blocking during the first simulation. Based on consideration of the simulation results, where less than 7.5% of the base material passed through the filter/was eroded in the first stage simulation, the combination was considered to lie within the "no erosion" categorization. Combinations where more than 7.5% of the base material was eroded in the first stage simulation and less than 7.5% was eroded in the second stage were classified as having "some erosion". "Continuing" erosion was considered to occur if more than 7.5% of the base material was eroded in both stages of the simulation. The repeatability was checked by rerunning selected simulations 10 times. The largest particle eroded did not change and the proportion eroded varied by no more than 5% of the total.

Examples of each classification can be seen in Fig. 13, which shows the percent of the total base material eroded against simulation time increment. Where some erosion occurs there is a significant drop in the amount of base material eroded between the first simulation and the second, which uses the partially blocked filter network which forms during the first simulation. By contrast, where continuing erosion occurs there is significant erosion in both simulations, and where no erosion occurs there is only negligible erosion.

In order to initially assess the validity of Terzaghi's filter rule [6] (i.e. to what extent PSD alone will control filtration), the results are presented against the D_{15F}/D_{85B} ratio. As a single D_{15F}/D_{85B} ratio can only be considered to be valid for a single relative density, the variation of base material which was eroded with the D_{15F}/D_{85B} ratio is

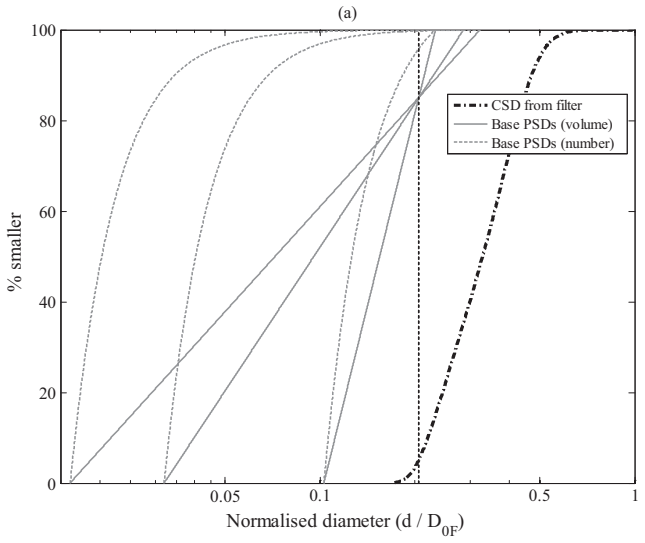

Fig. 11. Typical base-filter combination: Base PSDs: $D_{85B} = D_{c5}$ with Cu = 1.5, 3.0, 4.5.

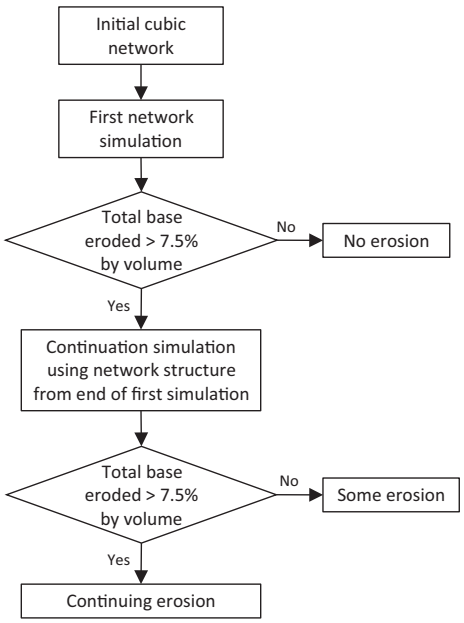

Fig. 12. Process to determine "no erosion", "some erosion" and "continuing erosion" filters.

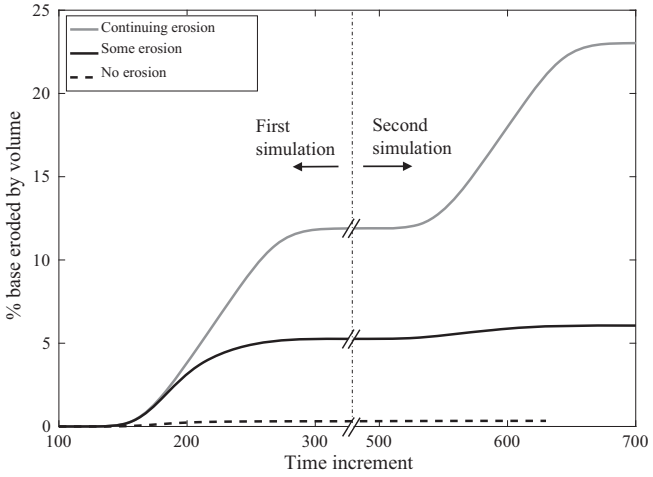

Fig. 13. Progression of continuing, some and no erosion simulations with time increments. Continuing erosion simulation is dense Cu_{filter} = 3.0, Cu_{base} = 1.5, $d_{85B} = D_{c5}$. Some erosion simulation is dense Cu_{filter} = 1.5, Cu_{base} = 3.0, $d_{85B} = D_{c5}$. No erosion simulation is loose Cu_{filter} = 1.5, Cu_{base} = 1.5, $d_{85B} = D_{c50}$.

considered in Fig. 14(a) for all filter-base combinations using loose filters and in Fig. 14(b) for dense filters. Results are coloured depending on the Cu_{base} of the material. Results for both the first and second simulations are shown and the 7.5% erosion limit used to define the boundary between no, some and continuing erosion. Although in general the proportion of base material eroded increases with D_{15F}/D_{85B}, as the filter density increases there is a clear reduction in the base material eroded for all combinations with $D_{15F}/D_{85B} > 5$. The proportion of base eroded is also highly dependent on Cu_{base}, with erosion generally reducing with increasing Cu_{base}. It is clear that even in idealized simulations such as those presented here the ratio D_{15F}/D_{85B} is insufficient to describe filter effectiveness and that where uncertainty exists other factors such as relative density must be taken into account.

Considering the loose filters, when $D_{15F}/D_{85B} < 5$ all combinations are considered to be no erosion and so in these simulations $D_{15F}/D_{85B} = 5$ can be taken as the boundary between the no and

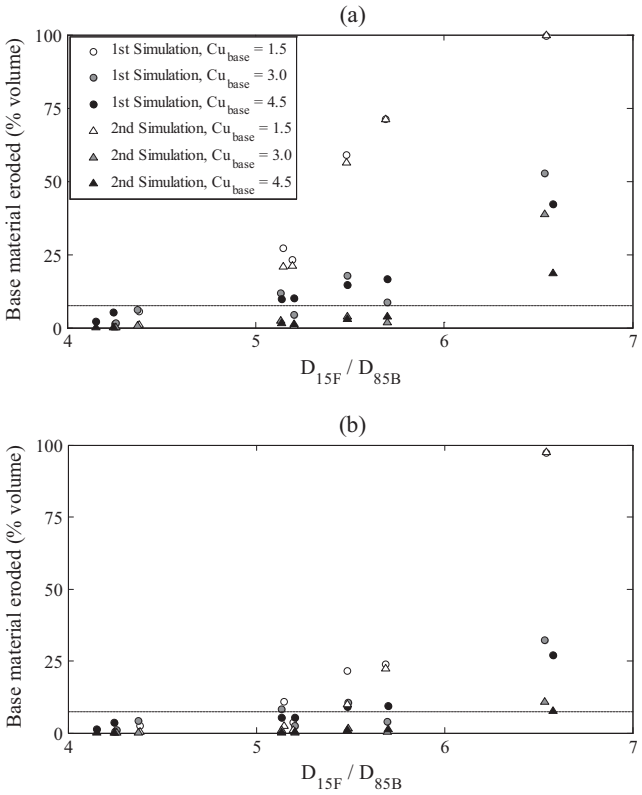

Fig. 14. Base material eroded in first and second simulations against D_{15F}/D_{85B} ratio: (a) loose filters; (b) dense filters.

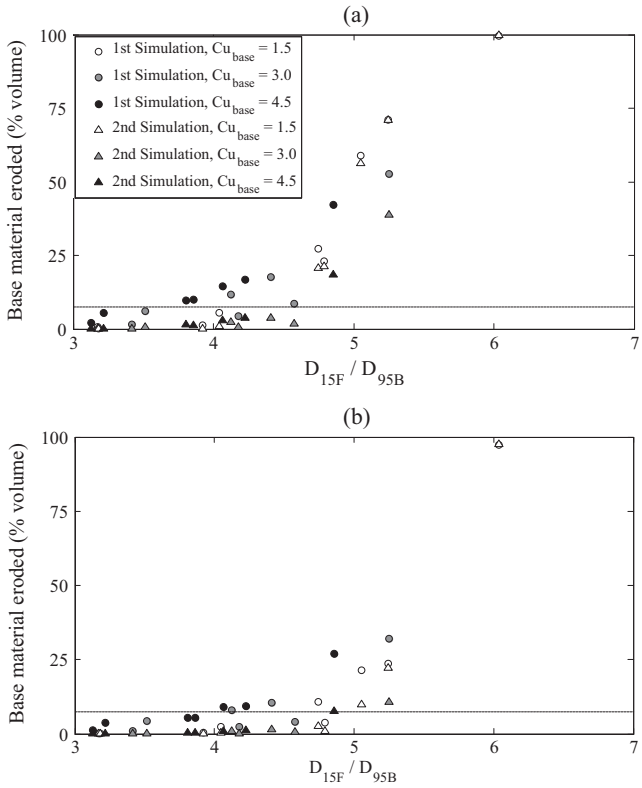

Fig. 15. Base material eroded in first and second simulations against D_{15F}/D_{95B} ratio: (a) loose filters; (b) dense filters.

some erosion filters. When $D_{15F}/D_{85B} > 5$ all base materials with $Cu_{base} = 1.5$ are classified as continuing erosion, although the proportion of base material eroded increases noticeably with D_{15F}/D_{85B} – when $D_{15F}/D_{85B} = 6.5$ almost all the base material is eroded. For each case where $Cu_{base} = 1.5$ there is only a small reduction in eroded material between the first and second simulations, showing that for the uniformly graded base material long-term clogging is less likely to occur. For base materials with $Cu_{base} = 3$ and 4.5, when $5 < D_{15F}/D_{85B} < 6$ all but one combination is classified as some erosion, meaning that the amount of eroded material reduces significantly between the first and second simulations as a greater proportion of constrictions are blocked at the start of the second simulation. The difference between the very uniform and more well-graded materials can be explained by the fact that, for a given D_{85B} the higher Cu_{base} materials have a larger D_{100B} and it is these larger particles which determine whether self-filtering will eventually occur.

When $D_{15F}/D_{85B} = 6.5$ and $Cu_{base} \geqslant 3.0$ there is a reduction in base material eroded between the first and second simulations, in particular for the simulation with $Cu_{base} = 4.5$ (from 43% to 18%). However, the amount of material eroded is still significant and it is likely that these samples are slowly clogging, rather than self-filtering close to the base/filter interface. This will be revisited later in the paper.

It can be seen in Fig. 14 that it is not possible to define a clear boundary between the some and continuing erosion categories using D_{15F}/D_{85B}. Foster and Fell [5] suggested that D_{15F}/D_{95B} was more effective than D_{15F}/D_{85B} for defining this boundary. Fig. 15 shows the relationship between D_{15F}/D_{95B} and the proportion of base eroded. It can be seen that a much clearer boundary between some and continuing erosion is defined at $D_{15F}/D_{95B} = 4.7$. Although this is a much smaller ratio that Foster and Fell's boundary, it shows a good qualitative agreement.

Fig. 16 examines the influence of the Cu_{filter} value by considering the loose filters and base materials with $Cu_{base} = 1.5$. Referring to Fig. 16(a), when normalised by D_{0F}, the largest particle eroded increases with Cu_{filter}. This corresponds to the increase in the CSD diameter as Cu_{filter} increases from 1.5 to 3, as shown in Fig. 7. However, when normalised by D_{15F} the size of the largest eroded particles is practically the same for both Cu_{filter} values at $D_{100B,eroded} = 0.2\ D_{15F}$ (Fig. 16(b)). This is in good agreement with the experimental work of Kenney et al. [4]. As illustrated in Fig. 16(c), for $Cu_{filter} = 1.5$ and 3 the relationships between the D_{15F}/D_{85B} ratio and the proportion of base material eroded are similar. The close agreement for filters normalised by D_{15F} is a consequence of the CSDs for the materials being similar when normalised by D_{15F}, as shown by in Fig. 7(c).

Up to this point there has been an emphasis on comparing the PSDs of the filter. However the filter density is known to influence the filter CSD [19,29]. Here, the influence of filter density can be appreciated by reference to Fig. 17 which considers the loose and dense CSDs for $Cu_{filter} = 1.5$ combined with a base with $Cu_{base} = 1.5$; D_{85B} was varied as discussed above. Referring to Fig. 17(a), the largest particle eroded is larger for the looser filter in all cases excluding the least effective combination where $D_{15F}/D_{85B} \geqslant 6.5$ (for this combination almost all the material is eroded in both cases). Shire and O'Sullivan [29] report that the constriction diameters are consistently around 10% smaller for the dense filters at a given % smaller value, and this is reflected in the change in $D_{100B,eroded}$ with density. The filter density clearly influences the filter performance, as shown in Fig. 17(b). For $D_{15F}/D_{85B} < 5$, both loose and dense filters are effective and only a small proportion of the base material is eroded. For intermediate values where $5 < D_{15F}/D_{85B} < 6$, the filter density has a marked effect on the filter effectiveness, considering both the volume of base material eroded and the size of the largest eroded particle.

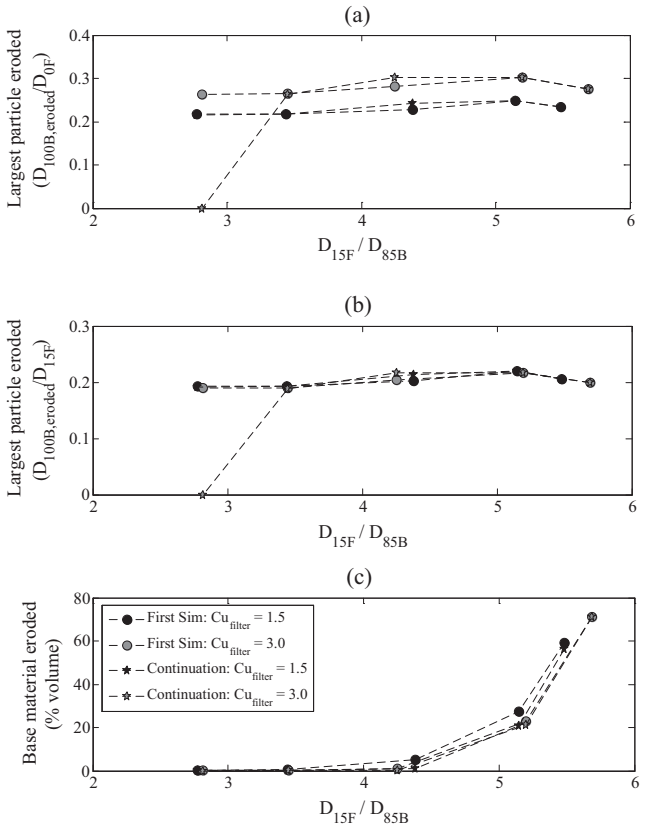

Fig. 16. Effect of Cu_{filter} on random walk results for loose filters: (a) variation of largest particle eroded with D_{15F}/D_{85B}; (b) variation of proportion of base material eroded with D_{15F}/D_{85B}; (c) variation of largest particle eroded normalised by D_{15F} with D_{15F}/D_{85B}.

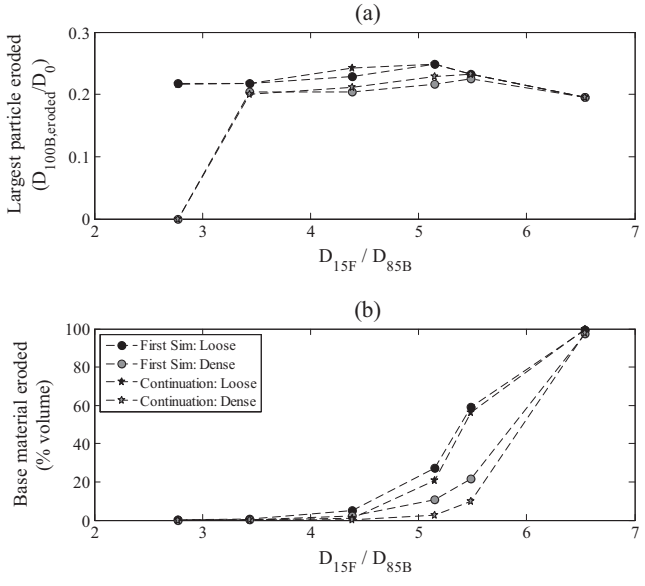

Fig. 17. Influence of filter relative density on network model results for $Cu_{filter} = 1.5$ and Cubase = 1.5: (a) variation of largest particle eroded with D_{15F}/D_{85B}; (b) variation of proportion of base material eroded with D_{15F}/D_{85B}.

The area-biased network model allows data on the pore-scale evolution of erosion and self-filtering to be recorded. Fig. 18 shows the development of the PSD of material retained in the filter as a typical network simulation progresses. During the first increment

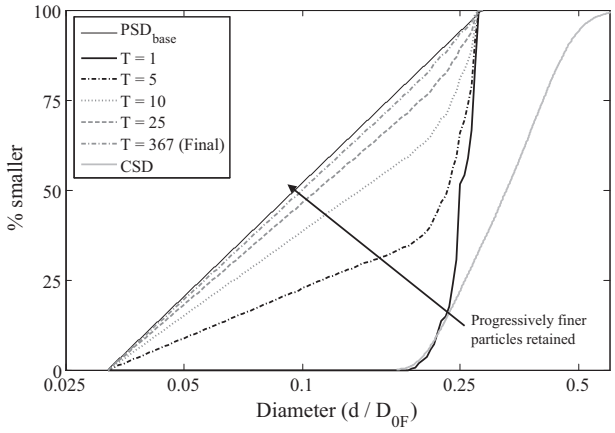

Fig. 18. Development of PSD of captured material during network simulation for loose filter with $Cu_{filter} = 1.5$, $Cu_{base} = 3$ and $D_{85B} = D_{c5}$.

a small number of base particles, which are all larger than the smallest constriction are retained. This causes a number of voids close to the filter entrance to become blocked, and as the simulation progresses these blocked voids are able to retain progressively finer particles. The network data are also able to demonstrate the hypothesis of [4] that self-filtering typically occurs within a thin layer close to the filter-base interface. Fig. 19(a) shows that there is no relationship between total proportion of base eroded and the proportion of constrictions which are blocked at the end of the second simulation. In fact, many of the samples with the least amount of base material eroded have only a small proportion of

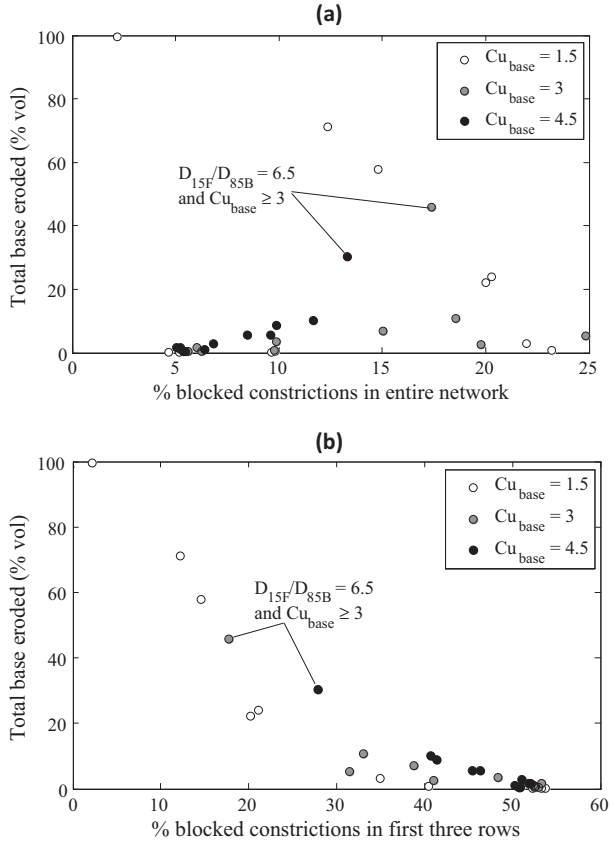

Fig. 19. Comparison of base material eroded (average of first and second simulations) for all loose filter samples: (a) constrictions blocked throughout network; (b) constrictions blocked in first three rows only.

Table 3
Effect of modifying void connectivity for simulation with Cu_{filter} = 1.5, Cubase = 1.5, $D_{85B} = D_{c5}$.

Void connectivity	Modified connectivity (non-cubic network with average connectivity = 6)				Original connectivity (regular cubic network with average connectivity = 6)		
	Proportion of voids with given connectivity (%)	Average base particles retained per void	All voids: Average base particles retained	Proportion of particles retained by voids of given connectivity (%)	Proportion of voids with given connectivity (%)	Average base particles retained per void	Proportion of particles retained by voids of given connectivity (%)
4	3.5	397	173	6.4	–	–	–
5	22.8	444		54.6	–	–	–
6	47.6	98		30.8	100	96	100
7	22.6	39		6.5	–	–	–
8	3.5	62		1.7	–	–	–

constrictions blocked (<7.5%). However, when the constrictions blocked within the first three layers of the filter only are considered (Fig. 19(b)) a clear relationship of decreasing erosion with increasing blocked emerges, showing that for a homogeneous filter only the constrictions close the entrance need to become blocked for self-filtering to occur [37].

A second process of clogging (a slow blocking of the filter) can also be identified from these results. As noted earlier, $D_{15F}/D_{85B} = 6.5$ and $Cu_{base} \geqslant 3.0$ there is a reduction in base material eroded between the first and second simulations. These samples have relatively a similar proportion of constrictions blocked in the first few rows as in the filter as a whole, suggesting a slow blocking process may be leading to the slow reduction in eroded material and eventual clogging of the filter.

Recognizing the potential sensitivity of the model and the results to the initial network connectivity, the base/filter combinations with Cu_{filter} = 1.5 (loose) were repeated for a network with the same average connectivity (six), but constrictions were created between diagonally neighbouring voids, or deleted until the connectivity distribution shown in Table 3 was reached. The sizes of the largest eroded particles did not differ significantly (the maximum diameter difference was 5.5%). However, as shown in Fig. 20, the percentage of base material eroded was greatly reduced when the modified connectivity was used. The voids with fewer than six connections appear to have a disproportionate effect on the system, as illustrated by the case for which Cu_{filter} = 1.5, Cu_{base} = 1.5 and $D_{85B} = D_{c5}$ in Table 3. The voids with fewer than six connections retain the majority of the base particles (61%) despite representing only 26.3% of the total voids. The application of the model presented isolated the effect of the CSD from other factors, such as void connectivity. However, this sensitivity analysis shows that future work should consider both CSD and the soil fabric by modelling void connectivity. Algorithms to produce large networks which can match the CSD and void connectivity distribution of real networks have been proposed e.g. [38,39].

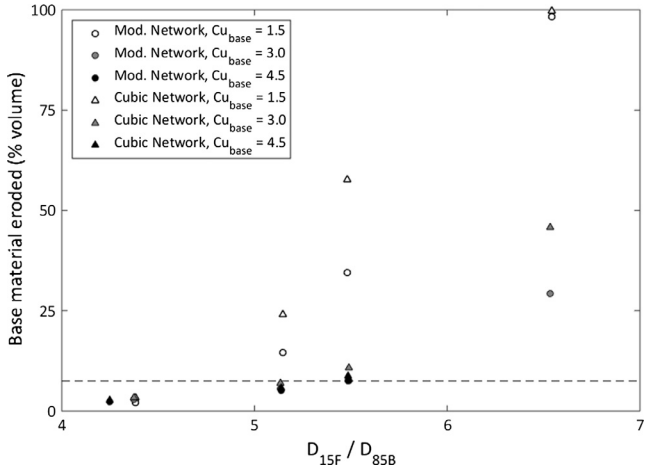

Fig. 20. Variation in material eroded with change in network connectivity.

7. Conclusions

This contribution has proposed a network model that uses an area-biased random walk approach to simulate the percolation of a finer base material through a given filter for a given filter constriction size distribution (CSD) (obtained from microCT or particle-scale simulation) and the base particle size distribution (PSD). Accurate particle-fluid coupled simulations of the filtration process with the millions of base particles required to get a representative model response is not currently possible. The abstractions adopted here to represent a physical system enabled up to 400 million base particles to be considered and facilitated numerical analyses of base-filter interaction leading to improved insight into the physical processes involved. The model uses a highly idealized directed cubic network of voids (i.e. each void is connected to six neighbouring voids). The complex hydraulics within a filter are not explicitly considered, rather the probability of a eroding base particle moving into a void is proportional to the area of the constriction connecting the voids. A polydisperse base PSD may be used in the model, allowing mechanisms such as self-filtering, where coarser transported base particles first block the constrictions of the filter and therefore prevent the loss of the finer base particles to be considered. Additionally, micro-scale variables such as the PSD of base material retained in the filter can be obtained. The model was validated using experimental data from Kenney et al. [4]; for equivalent systems the largest particle which could be eroded in the network model was in good agreement with the experimental findings.

In the current study 66 base-filter combinations were analysed using up to 400 million base particles per simulation. The filter CSDs were obtained by analysing the output from DEM simulations using the weighted Delaunay triangulation method. The results provided the following insight into filter performance:

(a) The "no erosion", "some erosion" and "continuing erosion" classifications proposed by Foster and Fell [5] to analyse the results of filter tests were applied to the results of the network model. Similar to the conclusions of Foster and Fell [5], the ratio D15F/D95B was found to best divide some/no erosion from continuing erosion tests, whereas D_{15F}/D_{85B} was found to best divide no erosion from some/continuing erosion.
(b) Using the network model with CSDs from coarse samples with Cu_{filter} = 1.5 and 3, it was found that the largest particle which could be eroded normalised by D15F of the filter (D100B, eroded/D15F) was similar and independent of the Cu_{filter} value. This gives further support to the use of characteristic diameters as a means to approximate a controlling constriction size in filter design.

(c) The relative density of the filter can have a significant effect on the base/filter combination effectiveness. An increase in relative density from "loose" to "dense" led the average constrictions in the CSD and the largest particle eroded in the network model to reduce by a similar magnitude. The amount of base material eroded was sensitive to filter relative densities for filters which allow some or continuing erosion ($D_{15F}/D_{85B} > 5$).

(d) For a given D85B, which is typically taken to be the characteristic particle size for base materials, a higher Cubase was more likely to lead to self-filter following some erosion. Lower Cubase materials tend to either self-filter with little erosion or suffer continuing erosion. This is because the largest particles control self-filtering.

(e) A change in network structure can affect the results of the network model and so future studies should consider both constriction sizes and void connectivity (soil fabric). A non-uniform void connectivity distribution leads to a reduction in the base material eroded compared to a uniform distribution. This is true, even when the average void connectivity is held the same. This is due to voids with fewer than average connectivity having a disproportionate effect on material retention.

Acknowledgements

We would like to thank the two anonymous reviewers for their thorough and helpful comments, which helped to improve the paper. The contribution of Dr. Kevin Hanley to the DEM modelling is gratefully acknowledged. The first author was funded by an EPSRC Doctoral Training Account. Data Statement: All data created during this research are openly available from the Zenodo (https://zenodo.org/).

References

[1] ICOLD. Bulletin on internal erosion of dams, dikes and their foundations, vol. 1, Paris; 2015.
[2] Fannin J. Karl Terzaghi: from theory to practice in geotechnical filter design. J Geotech Geoenviron Eng 2008;134:267–76. http://dx.doi.org/10.1061/(ASCE)1090-0241(2008)134:3(267).
[3] Reboul N, Vincens E, Cambou B. A computational procedure to assess the distribution of constriction sizes for an assembly of spheres. Comput Geotech 2010;37:195–206. http://dx.doi.org/10.1016/j.compgeo.2009.09.002.
[4] Kenney TC, Chahal R, Chiu E, Ofoegbu GI, Omange GN, Ume CA. Controlling constriction sizes of granular filters. Can Geotech J 1985;22:32–43. http://dx.doi.org/10.1139/t85-005.
[5] Foster M, Fell R. Assessing embankment dam filters that do not satisfy design criteria. J Geotech Geoenviron Eng 2001;127:398–407. http://dx.doi.org/10.1061/(ASCE)1090-0241(2001)127:5(398).
[6] Terzaghi K, Peck R. Soil mechanics in engineering practice. J. Wiley and Sons; 1948.
[7] Sherard JL, Dunnigan LP. Critical filters for impervious soils. J Geotech Eng 1989;115:927–47. http://dx.doi.org/10.1061/(ASCE)0733-9410(1989) 115:7(927).
[8] Vaughan P, Soares H. Design of filters for clay cores of dams. J Geotech Eng Div 1982;108:17–31.
[9] O'Sullivan C, Bluthé J, Sejpar K, Shire T, Cheung LYG. Contact based void partitioning to assess filtration properties in DEM simulations. Comput Geotech 2015;64:120–31. http://dx.doi.org/10.1016/j.compgeo.2014.11.003.
[10] To HD, Galindo Torres SA, Scheuermann A. Primary fabric fraction analysis of granular soils. Acta Geotech 2014;10:375–87. http://dx.doi.org/10.1007/s11440-014-0353-9.
[11] Dong H, Blunt M. Pore-network extraction from micro-computerized-tomography images. Phys Rev E 2009;80:36307. http://dx.doi.org/10.1103/PhysRevE.80.036307.
[12] Taylor HF, O'Sullivan C, Sim WW. A new method to identify void constrictions in micro-CT images of sand. Comput Geotech 2015;69:279–90. http://dx.doi.org/10.1016/j.compgeo.2015.05.012.
[13] Homberg U, Baum D, Prohaska S, Kalbe U, Witt K. Automatic extraction and analysis of realistic pore structures from µct data for pore space characterization of graded soil. In: Proc. 6th Int. Conf. Scour Eros., Paris. p. 345–52.
[14] Jang J, Narsilio GA, Santamarina JC. Hydraulic conductivity in spatially varying media-a pore-scale investigation. Geophys J Int 2011;184:1167–79. http://dx.doi.org/10.1111/j.1365-246X.2010.04893.x.
[15] Soria M, Aramaki R, Viviani E. Experimental determination of void size curves. In: Brauns J, Heibaum M, Schuler U, editors. Filters geotech hydraul eng. Rotterdam: Balkema; 1993. p. 43–8.
[16] Sjah J, Vincens E. Determination of the constriction size distribution of granular filters by filtration tests. Int J Numer Anal Methods Geomech 2013;37:1231–46. http://dx.doi.org/10.1002/nag.2076.
[17] Rege SD, Fogler HS. Network model for straining dominated particle entrapment in porous media. Chem Eng Sci 1987;42:1553–64. http://dx.doi.org/10.1016/0009-2509(87)80160-4.
[18] Schuler U. Scattering of the composition of soils. An aspect for the stability of granular filters. In: Lafleur J, Rollin A, editors. Geofilters '96, Montreal. Bitech Publications; 1996. p. 21–34.
[19] Locke M, Indraratna B, Adikari G. Time-dependent particle transport through granular filters. J Geotech Geoenviron Eng 2001;127:521–9. http://dx.doi.org/10.1061/(ASCE)1090-0241(2001)127:6(521).
[20] Witt KJ. Filtrationsverhalten und Bemessung von Erdstoff-Filtern, vol. 104. Heft: Institut für Bodenmechanik und Felsmechanik der Universität Karlsruhe; 1986.
[21] Semar O. Anwendung der Perkolationstheorie zur Analyse des suffosiven Partikeltransportes. Bauhaus Universität Weimar; 2010.
[22] Berkowitz B, Ewing RP. Percolation theory and network modeling applications in soil physics. Surv Geophys 1998;19:23–72. http://dx.doi.org/10.1023/A:1006590500229.
[23] Moraci N, Mandaglio M, Ielo D. A new theoretical method to evaluate the internal stability of granular soils. Can Geotech 2011;49:45–58. http://dx.doi.org/10.1139/t11-083.
[24] Silveira A, Peixoto T, Nogueira J. On void-size distribution of granular materials. Proc. 5th Pan-Amer conf soil mech found eng 1975:161–76.
[25] Taylor HF, O'Sullivan C, Sim WW. Geometric and Hydraulic Void Constrictions in Granular Media; 2016. <http://dx.doi.org/101061/(ASCE)GT1943-56060001547>.
[26] Plimpton S. Fast parallel algorithms for short-range molecular dynamics. J Comput Phys 1995;117:1–19. http://dx.doi.org/10.1006/jcph.1995.1039.
[27] Shire T, O'Sullivan C, Hanley KJ, Fannin RJ, O'Sullivan C. Fabric and effective stress distribution in internally unstable soils. J Geotech Geoenviron Eng 2014;140. http://dx.doi.org/10.1061/(ASCE)GT.1943-5606.0001184. 04014072.
[28] Barreto D. Numerical and experimental investigation into the behaviour of granular materials under generalised. Imperial College London; 2009.
[29] Shire T, O'Sullivan C. Constriction size distributions of granular filters: a numerical study. Géotechnique 2016. http://dx.doi.org/10.1680/jgeot.15.P.215. Published.
[30] Reboul N, Vincens E, Cambou B. A statistical analysis of void size distribution in a simulated narrowly graded packing of spheres. Granul Matter 2008;10:457–68. http://dx.doi.org/10.1007/s10035-008-0111-5.
[31] Sherard JL, Dunnigan LP, Talbot JR. Basic properties of sand and gravel filters. J Geotech Eng 1984;110:684–700. http://dx.doi.org/10.1061/(ASCE)0733-9410(1984)110:6(684).
[32] Honjo Y, Veneziano D. Improved filter criterion for cohesionless soils. J Geotech Eng 1989;115:75–94. http://dx.doi.org/10.1061/(ASCE)0733-9410(1989) 115:1(75).
[33] Tomlinson S, Vaid Y. Seepage forces and confining pressure effects on piping erosion. Can Geotech J 2000;37:1–13. http://dx.doi.org/10.1139/t99-116.
[34] Indraratna B, Raut AK, Khabbaz H. Constriction-based retention criterion for granular filter design. J Geotech Geoenviron Eng 2007;133:266–76. http://dx.doi.org/10.1061/(ASCE)1090-0241(2007)133:3(266).
[35] Lafleur J, Mlynarek J, Rollin A. Filtration of broadly graded cohesionless soils. J Geotech Eng 1989;115:1747–68. http://dx.doi.org/10.1061/(ASCE)0733-9410(1989) 115:12(1747).
[36] Gibson S, Abraham D, Heath R, Schoellhamer D. Bridging process threshold for sediment infiltrating into a coarse substrate. J Geotech Geoenviron Eng ASCE 2010;136:402–6. http://dx.doi.org/10.1061/(ASCE)GT.1943-5606.0000219.
[37] Witt K. Reliability study of granular filters. In: Brauns J, Heibaum M, Schuler U, editors. Filters geotech hydraul eng. Rotterdam: Balkema; 1993. p. 35–42.
[38] Idowu NA, Blunt MJ. Pore-scale modelling of rate effects in waterflooding. Transp Porous Media 2009;83:151–69. http://dx.doi.org/10.1007/s11242-009-9468-0.
[39] Jiang Z, van Dijke MIJ, Wu K, Couples GD, Sorbie KS, Ma J. Stochastic pore network generation from 3D rock images. Transp Porous Media 2011;94:571–93. http://dx.doi.org/10.1007/s11242-011-9792-z.